Independent Gating of Single Pores in CLC-0 Chloride Channels

Uwe Ludewig, Michael Pusch, and Thomas J. Jentsch
Center for Molecular Neurobiology, Hamburg University, D-20246 Hamburg, Germany

ABSTRACT The Cl^- channel from the *Torpedo* electric organ, CLC-0, is the prototype of a large gene family of Cl^- channels. At the single-channel level, CLC-0 shows a "double-barreled" behavior. Recently it was shown that CLC-0 is a dimer, and it was suggested that each subunit forms a single pore. The two protopores are gated individually by a fast voltage and anion-dependent gating mechanism. A slower common gating mechanism operates on both pores simultaneously. Previously, wild-type/mutant heteromeric channels had been constructed that display a large wild-type pore and small mutant pore. Here we use patch-clamp recording of single wild-type and mutant CLC-0 channels to investigate in detail the dependence of the gating of one protopore on the physically attached neighboring pore. No difference in rate constants of opening and closing of protopores could be found comparing homomeric wild-type and heteromeric wild-type/mutant channels. In addition, detailed kinetic analysis reveals that gating of single subunits is not correlated with the gating of the neighboring subunit. The results are consistent with the view that permeation and fast gating of individual pores are fully independent of the neighboring pore. Because the two subunits are associated in a common protein complex, opening and closing transitions of individual pores are probably due to only small conformational changes in each pore. In addition to the fast and slow gating mechanisms known previously for CLC-0, in the course of this study we occasionally observed an additional gating process that led to relatively long closures of single pores.

INTRODUCTION

Several genes coding for voltage-dependent Cl^- channels (CLC channels) have been cloned and functionally analyzed (Jentsch et al., 1990; for review see Pusch and Jentsch, 1994; Jentsch et al., 1995; Jentsch, 1996). CLC-0 and CLC-1 channels serve to stabilize the membrane potential in the *Torpedo* electric organ and skeletal muscle, respectively (Jentsch et al., 1990; Steinmeyer et al., 1991b). The broadly expressed CLC-2 channel is probably involved in cell volume regulation (Gründer et al., 1992) and is important for the control of intracellular Cl^- concentration in nerve cells (Staley et al., 1996). The importance of the muscular CLC-1 channel is underscored by its involvement in recessive and dominant myotonia (Steinmeyer et al., 1991a; Koch et al., 1992; George et al., 1993; Steinmeyer et al., 1994). Mutations in the homolog CLC-5 (Fisher et al., 1994; Steinmeyer et al., 1995) are responsible for Dent's disease, a hereditary kidney stone disease with associated proteinuria and hypercalciuria (Fisher et al., 1994; Lloyd et al., 1995).

The best characterized member of the CLC family is the voltage-gated Cl^- channel from *Torpedo* electric organ (CLC-0; Jentsch et al., 1990). This channel is known to have two different gating mechanisms of opposite voltage dependence. A fast gate (operating in the millisecond time range) opens CLC-0 at depolarized voltages with an apparent gating valence of ~1 elementary charge (Miller, 1982; Hanke and Miller, 1983). A much slower gating mechanism opens CLC-0 at hyperpolarizing voltages.

In early single-channel analysis of the *Torpedo* electric organ channel, Miller (1982) observed that the dwell times in the different conductance states are binomially distributed. Miller suggested that the channel has two pores in parallel, with each pore gated independently of the second pore (Miller, 1982). This "double-barreled" model, and a homodimeric structure of CLC-0 are now almost proven (Ludewig et al., 1996; Middleton et al., 1996). By using chemical modification of specific cysteine residues in mutant CLC-0 subunits, Middleton et al. (1996) showed that CLC-0 is a dimer of two subunits. Each CLC-0 subunit (in which a lysine was replaced by cysteine at position 519) could be functionally modified exactly twice by different methanethiosulfonate reagents (Middleton et al., 1996). Using concatamers of mutationally altered subunits, Ludewig et al. reached a similar conclusion. In addition, their data suggest that each subunit probably forms a single pore (Ludewig et al., 1996).

In contrast to fast gating, slow gating is not a simple superposition of single-monomer characteristics, but is a function of both subunits contributing to the channel (Ludewig et al., 1996). An involvement of subunit interactions in slow gating was also suggested, based on a very strong temperature dependence of slow gating and effects of the amount of expression in *Xenopus* oocytes (Pusch et al., 1997).

In a most simple picture, thus, CLC-0 can be considered as a dimer with two pores that conduct and gate independently of each other. The regions of the subunits that are

Received for publication 12 February 1997 and in final form 24 April 1997.

Address reprint requests to Dr. Michael Pusch, Center for Molecular Neurobiology, Hamburg University, Martinstrasse 85, D-20246 Hamburg, Germany. Fax: 49-40-4717-4839. Present address of M. Pusch: ICB, CNR, Via de Marini 6, I-16149 Genova, Italy. E-mail: pusch@barolo.icb.ge.cur.it.

© 1997 by the Biophysical Society

0006-3495/97/08/789/09 $2.00

involved in the association are likely to be involved in the slow gating process.

Although previous studies suggested an independence of the two pores, a slight departure from independence may not have been detected by the analysis used. Indeed, the independence of both pores in the *Torpedo* channel had been questioned in an earlier study (Labarca et al., 1985). Labarca et al. found evidence for a slight correlation in the fast gating of single protopores. First, in contrast to others (Miller, 1982; Hanke and Miller, 1983; Bauer et al., 1991), they found a double-exponential distribution of the dwell times of (especially the intermediate) current level (where exactly one pore is open). Second, a slight autocorrelation of the dwell times of the intermediate level was observed. Third, they observed that mean dwell times of specific conductance states depend on the preceding and following states.

In single-channel recordings of wild-type CLC-0, the gating transitions cannot be assigned to individual protopores, because they have equal conductance. This degeneracy complicates the analysis of a possible correlation of the two pores. The situation is different in heteromers of WT and mutant subunits, in which the two protopores have different conductances (Ludewig et al., 1996). Here we exploit this asymmetry to investigate whether opening and closing rates are dependent on the conductance state of the associated subunit. In addition, we analyze whether the duration of opening of single pores depends on the simultaneous open or closed time of the attached subunit. This allows us to estimate whether open times and/or closed times are correlated.

The fast gating of single pores is strongly dependent on the extracellular Cl^- concentration, and the voltage dependence is conferred by the permeant anion itself (Pusch et al., 1995; Chen and Miller, 1996). This differs fundamentally from gating models proposed for voltage-dependent cation channels in which a voltage-dependent conformational rearrangement of the protein is thought to confer voltage dependence on the channel proteins.

The intrinsic coupling of gating with the conduction process fits earlier results that the gating of the *Torpedo* Cl^- channel is dependent on the Cl^- ion gradient (Richard and Miller, 1990). The gating transitions showed an nonequilibrium behavior: bursts of the double-barreled channel activity started often with the simultaneous opening of both pores, and bursts were frequently terminated by closings from the intermediate conductance level (only one pore open). Such a violation of microscopic reversibility is only possible in the presence of an energy source which, in the absence of an electric potential, must be the electrochemical Cl^- gradient (Richard and Miller, 1990). Here, again using WT/mutant heteromers, we tested to see whether a similar violation of microscopic reversibility could also be seen within a single burst of channel openings, when the slow gate remains open.

MATERIALS AND METHODS

Molecular biology and electrophysiological measurements

CLC-0 wild-type, mutant S123T, and concatameric constructs have already been described (Ludewig et al., 1996). Briefly, mutations were introduced by recombinant polymerase chain reaction and verified by sequencing. In tandem constructs (WT-S123T and S123T-WT) the stop codon of the first subunit was deleted and constructs were ligated via an engineered *Spe*I site. This introduced four new amino acids between two subunits (GTTS). Capped cRNA was transcribed in vitro with the mMessage mMachine kit (Ambion, Austin, TX). *Xenopus* oocytes were prepared, injected, handled, and patch-clamped as described (Pusch et al., 1995; Ludewig et al., 1996). Single-channel experiments were performed using the inside-out configuration of the patch-clamp technique (Hamill et al., 1981) on oocytes from which the vitelline membrane had been removed shortly before the experiment. For patch clamping, oocytes were bathed in a solution containing (in mM) 100 (or 160) *N*-methyl-D-glucamine-HCl (NMDG-Cl), 2 $MgCl_2$, 5 HEPES, and 5 EGTA, pH 7.4. Pipettes were filled with a solution containing (in mM) 95 NMDG-Cl, 5 $MgCl_2$, and 5 HEPES, pH 7.4. Data were low pass filtered with an eight-pole Bessel filter at 300 Hz (S123T mutant) or 500 Hz (other constructs), digitized at a higher frequency to avoid aliasing, and stored on a digital tape.

Data analysis

Analysis was performed with the Analysis 3.2x program (Biopatch, Biologic) and several home-written programs in QickBasic (Microsoft). Data were then further processed with the SigmaPlot program (Jandel Scientific, Corte Madera, CA).

For the kinetic analysis in Fig. 2, idealized current traces (>300 events) were constructed by employing a 50% threshold criterion, followed by visual inspection of each transition. From this, mean dwell times were determined (τ_{cc}, τ_{oc}, and τ_{oo} for homomeric channels; τ_{cC}, τ_{oC}, τ_{cO}, and τ_{oO} for heteromeric channels). For homomeric channels, opening rate α and closing rate β were calculated as $\alpha = 1/(2*\tau_{cc})$, and $\beta = 1/(2*\tau_{oo})$. Because open WT pores have an increased noise level, openings of the small mutant pore on top of open WT pores were less reliable than openings with closed WT pores. Therefore the gating rates were obtained using the following procedure. First we determined the well-defined dwell times of the lumped states τ_{cC+oC} and τ_{cO+oO} (i.e., ignoring transitions of the small mutant pore), from which we calculated $\alpha_{WT} = 1/\tau_{cC+oC}$, $\beta_{WT} = 1/\tau_{cO+oO}$. τ_{cC+oC} is the mean dwell time of closings of the large pore, irrespective of transitions of the small pore; τ_{cO+oO} is the mean dwell time of openings of the large pore, irrespective of transitions of the small pore. Using these values, we obtained α_{Mutant} and β_{Mutant} from τ_{cC} and τ_{oC}, assuming that $\tau_{cC} = 1/(\alpha_{WT} + \alpha_{Mutant})$ and $\tau_{oC} = 1/(\alpha_{WT} + \beta_{Mutant})$.

For recordings of single heteromeric channels, two idealized records corresponding to the gating transitions of the large and the small pore, respectively, were constructed by the following procedure. By using a 50% threshold criterion, events of the wild-type conductance level were detected. Then the data were smoothed by replacing each ordinate data value by the mediate value of two to four neigboring ordinate data points, depending on the noise level of the original data. This procedure was necessary to reduce the flickery noise of open WT pores. The smoothed current recording was idealized with a 50% criterion, followed by visual inspection of each transition. This leads to a reduced time resolution for the smaller transitions of the mutant pore, which is justified, however, by the fact that gating of the mutant pore is more than two times slower than the WT pore.

The autocorrelation coefficient $G(k)$ of open or closed dwell times as a function of neighboring events $k = 1, 2, 3, \ldots$ was calculated with the

following formula (Labarca et al., 1985):

$$\Gamma(k) = \sum_{i=1}^{n-k}(\tau_{i+k} - \tau_{mean})(\tau_i - \tau_{mean}) / \sqrt{\Sigma_{i=1}^{n}(\tau_i^2 - \tau_{mean}^2)} \quad (1)$$

with

$$\tau_{mean} = \frac{1}{n}\sum_{i=1}^{n}\tau_i \quad (2)$$

where n is the number of all events in the investigated current level; k is the number of the first, second, third, . . . neighboring current level; and τ_i is the dwell time in that level of event i.

The dwell-time histograms were constructed and displayed as suggested by Sigworth and Sine (1987).

Several kinds of analysis were performed to look for correlations in the gating of heteromers. To investigate the (in)dependence of opening and closing rates on the following state, we did the following. Two dwell-time histograms for both the open and the closed dwell times of the large pore were constructed. Each contained only events that were attributed to one of the states in Fig. 6 *A*. From that, we calculated the opening rates $\alpha_1 = \alpha_{S123T\ open}$ and $\alpha_2 = \alpha_{S123T\ closed}$ by $\alpha_1 = 1/\tau_{Co}$ and $\alpha_2 = 1/\tau_{Cc}$. The closing rates were calculated by $\beta_1 = 1/\tau_{Oo}$ and $\beta_2 = 1/\tau_{Oc}$.

To investigate the possibility that simultaneous open times of the large pore and the small pore in heteromeric channels were correlated, we performed the following analysis. Openings of the small pore were divided into three groups of different duration (short, intermediate, and long). For each open event of the small pore, we selected all simultaneous openings of the large pore, even if they overlapped only partially. By this method we assigned most of the open events of the large pore to three different groups (short, intermediate, and long) of open times of the small pore. Events of the large pore that had no simultaneous openings of the small pore were not counted. Some events of the large pore will be assigned to more than one small pore open time interval, because it overlapped with two or more large pore open dwell times. Because long openings of the WT pore, especially with longer openings of the small pore, have a priori a higher chance of overlap, each event had to be corrected for this probability to obtain an unbiased histogram of WT openings for each group. In the absence of correlation, the probability of an overlap by at least one sample point of a large pore opening of length t_W (in sample times) and a small pore opening of length t_M in a record of N sample points is

$$p_x = (t_W + t_M - 1)/N$$

if $t_W \ll N$, and $t_M \ll N$. Therefore, for a given pair of openings, (t_W, t_M), the bin in the corresponding histogram of the WT open times was augmented by $1/p_x$. These "weighted" histograms were then scaled by an arbitrary factor.

All fits were performed by using a least-squares minimization procedure.

RESULTS

Gating of wild-type and mutant CLC-0 channels

Wild-type (WT) and mutant CLC-0 were expressed in *Xenopus* oocytes, and single channels were recorded in the inside-out patch configuration (Hamill et al., 1981). WT has a conductance of ~8 pS, and dwell times in the various states are in the 1–10-ms time range (Fig. 1 *A*). Transition rates between the conductance levels are voltage dependent, leading to a voltage-dependent open probability of the channel. The dwell times in all three conductance levels are binomially distributed, suggesting that the two conductance levels are gated independently (Miller, 1982; Bauer et al., 1991). In addition to these fast gating transitions shown in Fig. 1 *A*, single-channel recordings display long stretches of missing channel activity, which indicate the simultaneous closing of both pores by the slow gate (not shown).

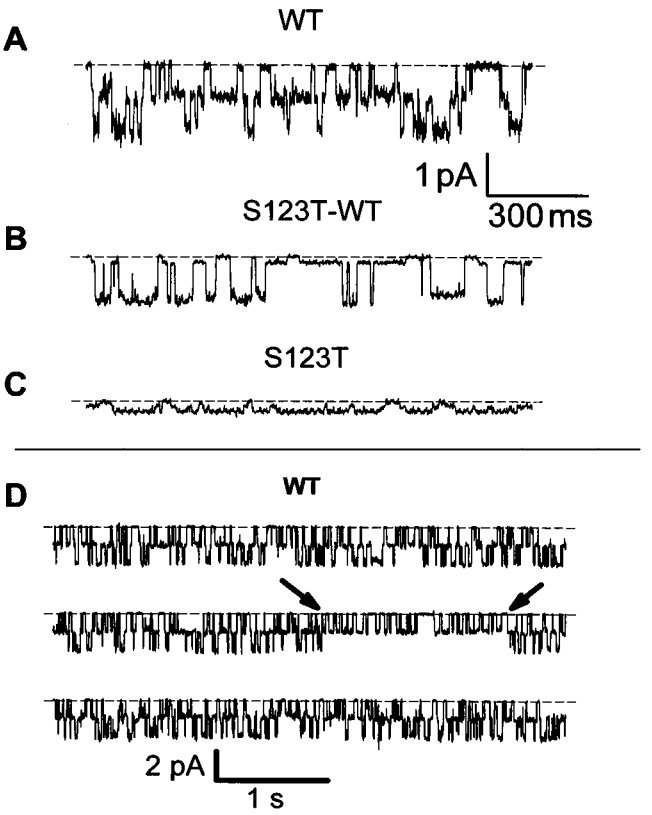

FIGURE 1 Single-channel current traces for a CLC-0 wild-type dimer (*A*), a S123T wild-type dimer (*B*), and mutant S123T at −100 mV (*C*). (*D*) Continuous single-channel recording from CLC-0 wild type at −140 mV, showing very rare events (<0.05% of the time) of slow closings of an individual pore. Note the 1.5 s (indicated by *arrows*) in which a maximum of one pore opened. During this period the open probability of the remaining pore is 0.50, exactly the same value that was calculated for one of both channels in the remaining time. Dashed lines indicate zero current.

The point mutant S123T has a conductance of ~1.5 pS and slower gating kinetics (Ludewig et al., 1996; Fig. 1 *C*). A concatamer of the mutant and WT (S123T-WT) shows a double-barreled behavior with a WT (8 pS) and a mutant (1.5 pS) pore (Ludewig et al., 1996; Fig. 1 *B*).

In addition to the fast and slow gating described so far, we detected a third type of gating process. Occasionally, during a burst of channel activity, one of the two protopores closes for a relatively long time, whereas the remaining pore continues to gate with the same open probability as before (Fig. 1 *D*). Such closures cannot be attributed to the slow gate that operates on both pores simultaneously (because only one pore is closed), or to the fast gate (because the closure is too long). Such events were also detected in S123T mutant and S123T-WT concatameric channels (data not shown). Thus we must conclude that an additional gating mechanism is present in CLC-0, a slow gate that operates on single protopores. Closures due to this third gate

tended to occur more often at very negative voltages. However, because such events occurred only very rarely, we did not analyze the process in detail. It could be neglected for the following analysis.

We used several strategies to test for a possible correlation of the fast gating of the two protopores. First, we investigated whether parameters of fast gating are dependent on the nature of the second pore, i.e., if gating rates are different in homomeric or heteromeric channels. Second, triggered by the results of a previous report (Labarca et al., 1985), we looked for autocorrelations in pure WT channels. Third, we exploited the asymmetry of heteromeric channels to reveal any correlation of the two pores. In a last type of analysis, we used the heteromeric channels to test for a violation of microscopic reversibility restricted to the fast gating process.

For homomeric channels, assuming two independent pores of equal conductance, gating rates can be determined from single-channel recordings, as first described by Miller (1982). Because the two pores are identical, gating rates are overdetermined in such an analysis (Miller, 1982; Hanke and Miller, 1983). Gating of wild type is nicely described by this binominal model (data not shown), and resulting gating rates are shown in Fig. 2 *A* (*filled symbols*). For heteromeric channels (Fig. 1 *B*), opening and closing rates of the two different pores can be obtained as described in Materials and Methods.

Fig. 2 *A* illustrates that opening and closing rates for the large WT pore in homomeric WT channels (Fig. 2 *A*, *filled symbols*) are very similar to the corresponding rates of the large WT pore in the context of heteromeric channels (Fig. 2 *A*, *open symbols*). The opening and closing rates of the (more difficult to measure) small S123T pore are also very similar in homo- and heteromeric channels (Fig. 2 *B*). Thus the rate constants of the fast gate are independent of the nature of the physically attached pore.

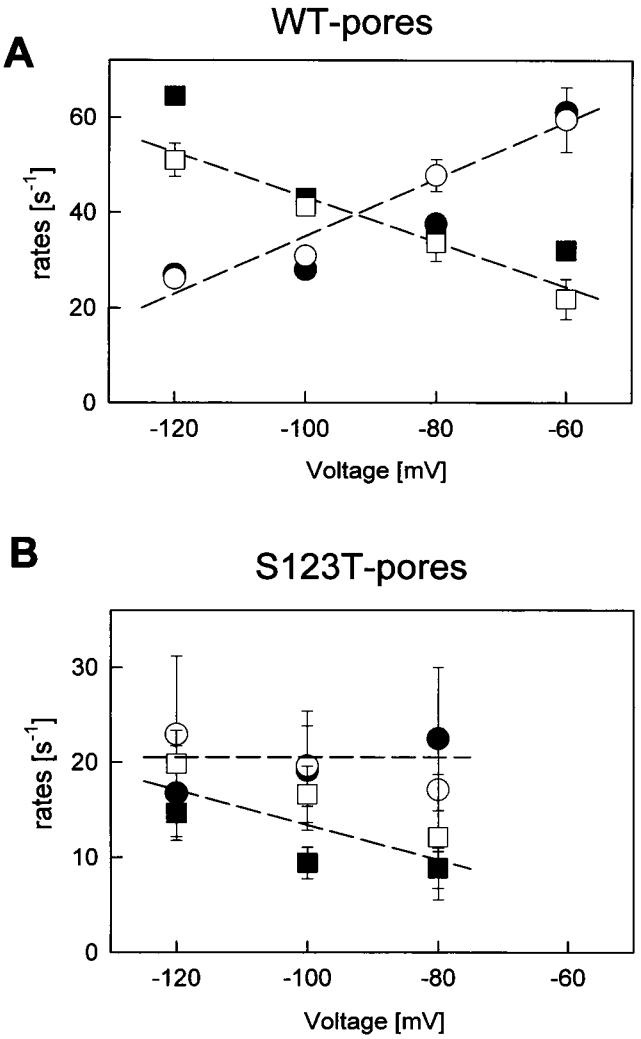

FIGURE 2 Opening and closing rates as a function of voltage. (*A*) Opening rates (α) of homomeric wild-type pores (●) have values nearly identical to those of wild-type pores in heteromeric S123T/WT-dimers (○). Closing rates (β) of homomeric wild-type pores (■) behave similar to wild-type pores in heteromeric S123T/WT-dimers (□). (*B*) Opening rates of homomeric S123T pores (●) and S123T pores in heteromeric S123T/WT-dimers (○), and closing rates of homomeric S123T pores (■) and S123T pores in heteromeric S123T/WT-dimers (□). Dashed lines indicate the tendency of voltage dependence and are drawn by eye.

Absence of correlations in wild-type CLC-0

The results described above favor the view of a gating mechanism that operates independently on each pore of the "double-barreled" channel. However, correlations in the gating of single subunits cannot be rigorously excluded. In fact, the independence of protopores had been questioned by Labarca et al. (1985), who described several indications for a correlation of single pores in wild-type gating. Because correlation analysis is complicated by the degeneracy of the WT double-barreled channel, we sought to exploit the asymmetry of the heteromeric constructs to rigorously test the independence of single protopores. First, we performed an analysis similar to that of Labarca et al. (1985), which was also performed on homomeric WT channels.

Fig. 3 *A* shows, typically for the intermediate conductance level, that the dwell-time distribution can be nicely fitted with a simple exponential function. When the dwell times are binned logarithmically and displayed in the Sigworth and Sine (1987) convention, one would expect a single peak of the the dwell-time distribution for a monoexponential process, as is indeed found (Fig. 3 *B*). In contrast to this result, Labarca et al. (1985) had found a double-exponential distribution for the intermediate conductance level. A possible explanation for this discrepancy will be discussed below.

An estimate for correlations in the gating of single pores can be obtained by calculating the autocorrelation coefficient as a function of the neighboring dwell times (see Eq. 1 and Labarca et al., 1985). Such an analysis is shown in Fig. 3 *C* for the intermediate conductance level. No correlation can be seen. We could not find a correlation of dwell

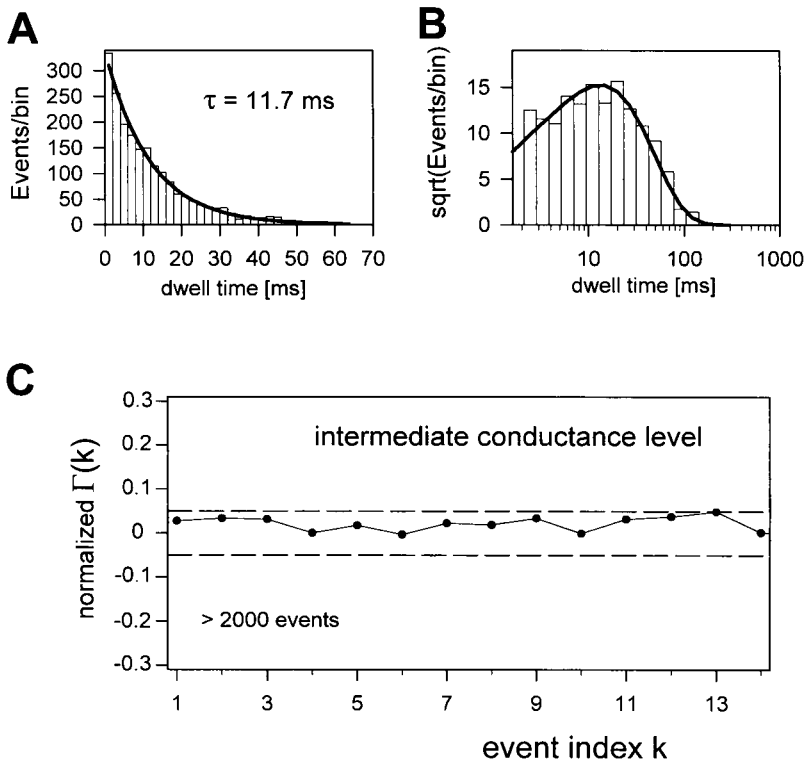

FIGURE 3 Monoexponential kinetics and absence of autocorrelation in WT fast gating. (*A* and *B*) Dwell-time histograms for the intermediate conductance level at −140 mV in a linear (*A*) and a Sigworth and Sine (*B*) display. (*C*) Autocorrelation for the intermediate current level in wild type at −140 mV. At this potential the channel has an open probability similar to that of the channels analyzed by Labarca et al. (1985) at higher Cl^- concentrations. The autocorrelation was calculated from Eq. 1. A positive correlation at a certain index, *k*, means that, on average, the *n*th opening is correlated with the (*n* + *k*)th opening, i.e., the two have a similar duration. Similar results were observed in five different patches.

times (as a function of neighboring dwell times, *k*) for any of the the three conductance states in wild-type CLC-0 at −100 mV, −120 mV, and −140 mV. Again, this result is in contrast to the observations of Labarca et al. (1985), who detected a slight correlation (~0.1) of the intermediate conductance level at very negative voltages. This discrepancy will be discussed below.

Absence of correlations in heteromeric CLC-0 channels

The individual opening and closing transitions of single pores can be monitored in heteromeric (S123T/WT) channels with two different conductances (Figs. 1 *B* and 4 *A*). This makes it possible to analyze whether transitions of individual pores influence the gating of the attached pores.

In a first analysis, we determined opening and closing rates of the large WT pore, depending on the state of the small pore at the time of the transition (see Fig. 4 *A*). Examples are shown in Fig. 4 *B* for the open time (from which the closing rate is determined) and in Fig. 4 *C* for the closed time (from which the opening rate is determined). In all cases, distributions can be nicely fitted with single-exponential functions. Results from several experiments at −120 mV with 160 mM internal chloride reveal α_1 = 19.4 ± 2.8 s^{-1}, α_2 = 18.2 ± 3.6 s^{-1}, β_1 = 40.7 ± 5.2 s^{-1}, and β_2 = 33.1 ± 5.0 s^{-1} (mean ± SD). Thus both opening as well as closing rates of the WT pore are almost independent of the preceding conductance state of the associated small pore.

In principle, it is conceivable that long open times of the large pore correlate with simultaneous long open times of the small pore. In this case, long open times (and short open times) of individual pores would be clustered. Another possibility is that long open times of one pore tend to be associated with simultaneous short open or closed times of the other pore. Such correlations could have been overlooked by the previous analysis. To reveal possible correlations of this type, we performed the following analysis.

Openings of the small pore were divided into three groups: short openings (duration < 17 ms), intermediate openings (duration between 17 ms and 72 ms), and long openings (duration > 72 ms). Then, for each opening of the small pore, we selected all openings of the large pore that partially overlapped with the chosen opening of the small pore. In this way, we get three different groups of openings of the large pore. Openings of the large pore that do not overlap with any opening of the small pore are not counted, and long openings of the large pore will be counted with higher a priori probability. Correcting for this latter bias (as described in Materials and Methods), we arrive at normalized open time histograms for the large pore for each of the three groups of openings of the small pore, as shown in Fig. 5.

If long openings of the small pore are preferentially simultaneous with long openings of the large pore (or vice versa), the mean open time estimated from the thus obtained histograms should differ for the different groups. We get, however, very similar mean open times for all three different histograms. Performing the same kind of analysis with

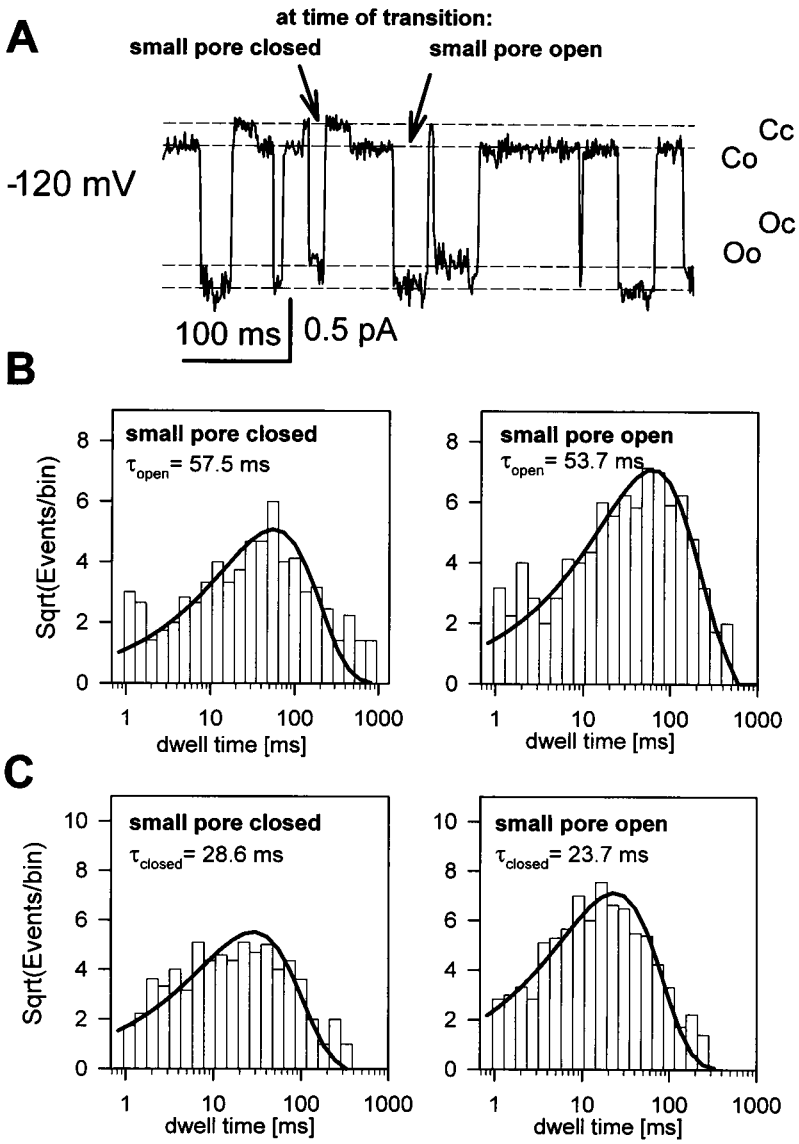

FIGURE 4 (*A*) Single-channel trace of S123T-WT dimer with examples for the dwell time in individual states that were counted. (*B*) Examples for dwell-time histograms of a 60-s trace before opening depending on the state (Cc → Oc transition) and (Co → Oo transition). (*C*) Examples for dwell-time histograms before closing (Oo → Co transition) and (Oc → Cc transition). Histograms in *B* contain 457 and 241 events, respectively, and those in *C* 448 and 274 events, respectively.

the closed times of the large pore also did not reveal any dependence of the mean closed time on the associated open times of the small pore (data not shown). In conclusion, we could not detect any dependence of the kinetic behavior of the large pore on the state of the associated small pore.

Microscopic reversibility of fast gating in heteromeric CLC-0 channels

The two pores have different conductances in a heteromeric channel; thus we can identify openings of individual wild-type or mutant pores. The channel can either be fully open (Oo), fully closed (Cc), or exactly one of the pores can be open (Oc or Co; Fig. 6 *A*). The channel can be also inactivated for longer time stretches; this adds an additional closed state to the picture (Cc_{slow}; Fig. 6 *A*). Cc and Cc_{slow} are both nonconducting and are therefore not directly distinguishable. The situation is shown in the Markov diagram in Fig. 6 *A*: with the slow gate open, each pore can individually open and close, while the slow gate operates simultaneously on both pores.

We now concentrate on the gating within bursts of openings, and thus the gating between states Oo, Oc, Co, and Cc. If the pores are fully independent, one would expect to find that there is no preference for a clockwise or counterclockwise cycling within the state diagram of Fig. 6 *A*, i.e., microscopic reversibility holds. Schematic examples of fast gating events that represent a clockwise or counterclockwise cycle within the state diagram of Fig. 6 *A* are shown in Fig. 6 *B*. Clockwise and counterclockwise cycles are indistinguishable in the wild-type channel, because the two intermediate conductance levels are identical.

In several single-channel patches of tandem S123T-WT or WT-S123T constructs without long closed times (due to the "slow" gating), we counted the clockwise and counterclockwise cycles, respectively (Fig. 6 *C*). No statistically

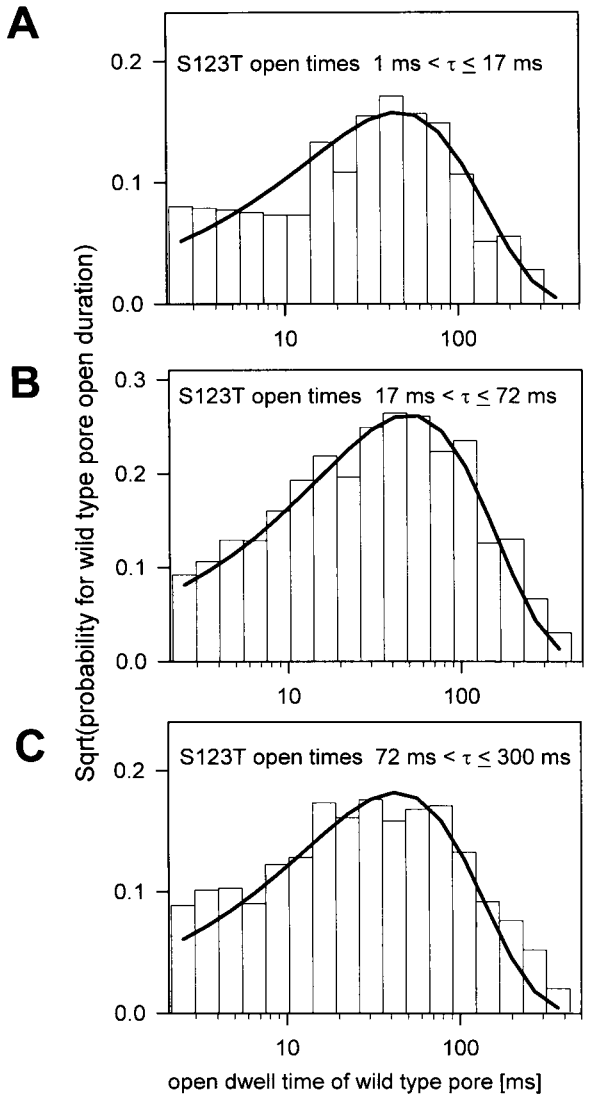

FIGURE 5 Mean open durations do not depend on open durations of the attached opening. Openings of the large conductance level were assigned to three different time windows: (*A*) 1 ms < $\tau_{S123T} \leq$ 17 ms; (*B*) 17 ms < $\tau_{S123T} \leq$ 72 ms; (*C*) 72 ms < $\tau_{S123T} \leq$ 300 ms of simultaneous openings of the small conductance level (at −120 mV). (See Materials and Methods and text for a detailed description of the analysis.) All three probability density functions peak at the same time constant, indicating that mean open times of the WT pore do not depend on the open duration of the attached S123T pore.

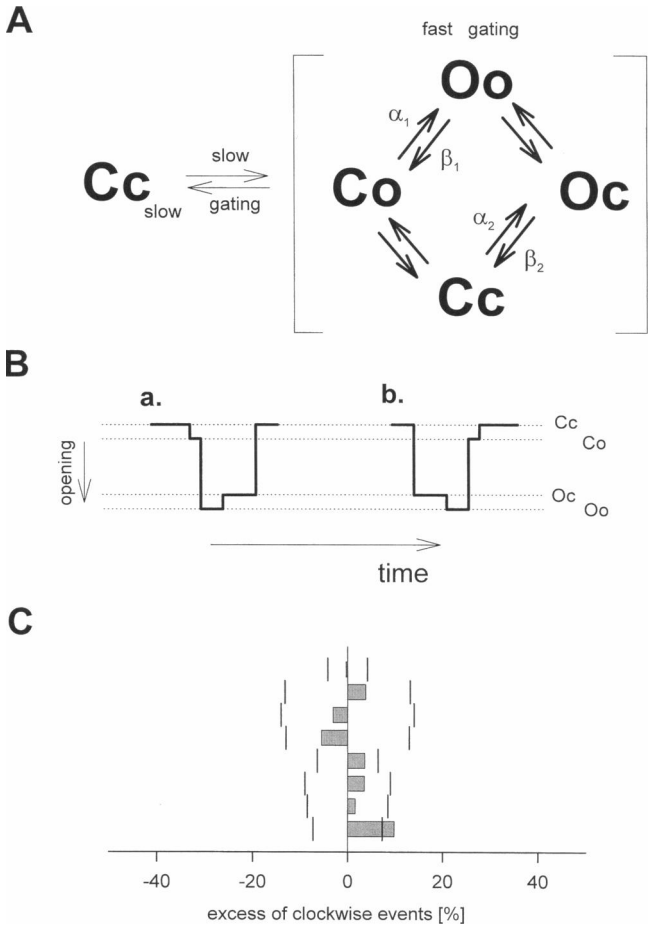

FIGURE 6 (*A*) Markovian five-state model for the gating of CLC-0, as proposed originally by Miller (1982). Rate constants of fast gating are indicated only for one of the two pores. For WT, states Co and states oC cannot be distinguished, and the equality $\alpha_1 = \alpha_2$ and $\beta_1 = \beta_2$ holds. For heteromeric channels, states Co and Oc have different conductances, and the opening/closing rate of the WT pore could, in principle, depend on the conductance state of the mutant pore, i.e., the above equalities do not necessesarily hold. (*B*) Possible events that represent clockwise (*a*) or counterclockwise (*b*) cycling in the right part of the state diagram shown in *A*. Microscopic reversibility is fulfilled if clockwise cycling and counterclockwise cycling occur with the same frequency. (*C*) Heteromeric fast gating channels obey the principle of microscopic reversibility. The number of clockwise (N_+) and counterclockwise (N_-) events was counted. The relative cycling excess was calculated as $(N_+-N_-)/(N_++N_-)$ and plotted for several different patches on top of each other. Small vertical lines indicate the 5% range of deviation that would be expected by statistical fluctuation (depending on the number of events). With this criterion, only one of eight channels (*bottom*) showed significantly more clockwise events than statistically expected.

significant preference for one direction can be seen. Thus, as expected, in the virtual absence of slow gating the principle of detailed balance holds for the states within the gating scheme of Fig. 6 *A*.

This result does not imply that fast gating of a single protopore is at thermodynamic equilibrium. Indeed, if chloride acts as the gating charge in CLC-0, as suggested by Pusch et al. (1995), fast gating is expected to be a nonequilibrium process violating detailed balance. This cannot be resolved, however, because the states of different ion occupancy of closed and open protopores (these states are not distinguished in the scheme of Fig. 6 *A*) cannot be measured directly.

DISCUSSION

In the present work we investigated the independence of the fast gating events of individual protopores in the double-barreled CLC-0 channel. To a first approximation, independence was suggested by the good description provided by

the simple binomial model, as was first demonstrated by Miller and colleagues (Miller, 1982; Hanke and Miller, 1983) and confirmed for the cloned channel (Bauer et al., 1991). Yet small deviations from independence, especially correlations of the two pores, could have been overlooked by the previous analysis.

The asymmetry of heteromeric channels allowed us to study the gating of individual protopores in much more detail. Several different approaches were applied to reveal possible correlations of the fast gating of the two pores of the channel. Analysis of homomeric WT gating similar to that performed previously (Labarca et al., 1985) did not show any evidence of a correlation. Moreover, several strategies applied to mutant/WT concatamers did not reveal any signs of interdependence of the two pores.

Our results, especially the analysis of homomeric WT gating, are in contrast to the findings of Labarca et al. (1985). These authors found evidence of a slight correlation in the fast gating of single protopores. Notably, a second, very fast component in the dwell-time histogram of the intermediate current level and a slight autocorrelation in an analysis of the type shown in Fig. 3 *C* were found. A possible reason for this discrepancy could be caused by the different experimental conditions used by Labarca et al. They had measured CLC-0 in 500 mM Cl^- (versus our 100 or 160 mM). This leads to a higher open probability of channels at negative potentials (Pusch et al., 1995; Chen and Miller, 1996; Ludewig et al., 1997). Probably most importantly, the different cutoff filter frequency used by Labarca et al. (2 kHz versus 500 Hz in this study) may explain the divergent results. In principle, a higher time resolution should be favorable. However, fast processes that are unrelated to the actual gating process are more likely to interfere with the analysis at higher filter frequencies. Indeed, we observed a rather high open channel noise for WT CLC-0 (Figs. 1 *A* and 7 *A*). The increased noise level of open channels could be caused by a flickery block or by a fast process intrinsic to the protein. Such a fast process must be evaluated with additional states in the gating scheme and could lead to additional short time constants of dwell-time histograms.

To estimate the apparent effect of such a fast process on correlation analysis, we modeled a simple fast blocking/gating process, as shown in Fig. 7, *B* and *C*. Normal fast gating of individual protopores was first simulated as a simple two-state process, O ↔ C, with rate constants similar to the ones measured experimentally (see Fig. 2 *A*). Two such simulated single-channel traces were added to obtain a "doubel-barreled" channel. Noise was recorded at a 10-kHz bandwith from the patch-clamp amplifier (without pipette) and added to the ideal simulated records. This "raw" current trace was filtered digitally at either 2 kHz (as in Labarca et al., 1985) (Fig. 7 *B*, *upper trace*) or at 500 Hz (as was done in this study) (Fig. 7 *B*, *lower trace*). The currents were analyzed as described in Materials and Methods, and a correlation analysis similar to the one shown in Fig. 3 was performed. No correlation is visible at either filter frequency

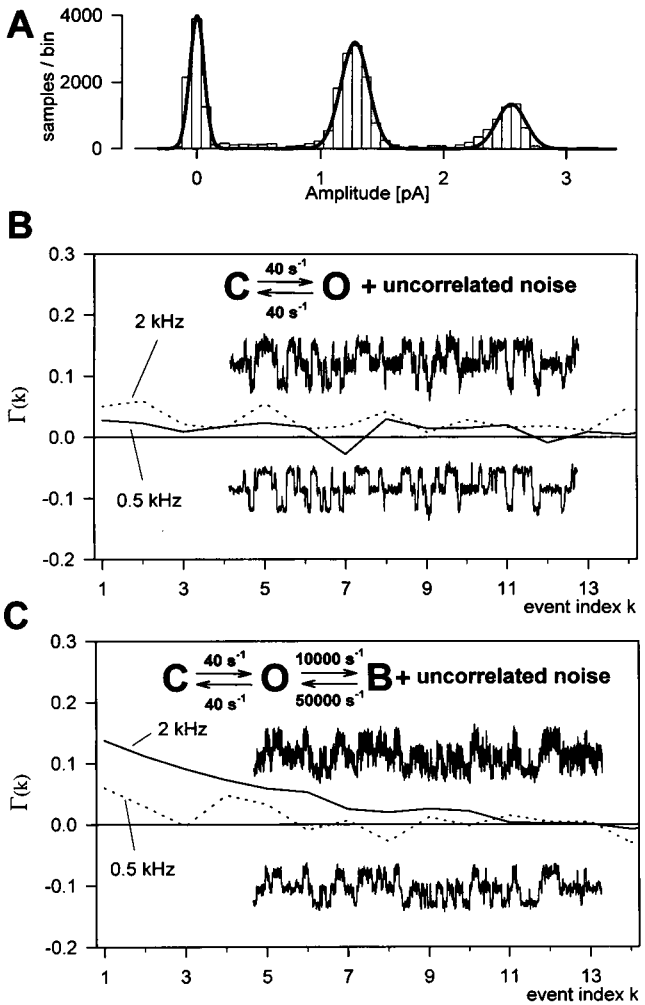

FIGURE 7 (*A*) Amplitude histogram of WT CLC-0, displaying the increased noise level of open pores compared to the noise level of the closed level. (*B*) Autocovariance of simulated noisy traces with one open and one closed state filtered at 2 kHz and 0.5 kHz. (*C*) Autocovariance of simulated noisy traces with an additional very fast block/gating on top of open events filtered at 2 kHz and 0.5 kHz. The very fast block is smoothed out by filtering, but with a filter corner frequency at 2 kHz, a small autocovariance remains that is not observed with higher (0.5 kHz) filtering. A total time of 60 s was simulated. The insets show a 1-s stretch of the simulated current.

in the absence of a fast blocking process (Fig. 7 *B*). The same procedure was then performed after a fast open-channel blocking process (Fig. 7 *C*) was added, using the same amplifier noise as before. In the presence of the fast process, an apparent correlation for $k \leq 4$ is visible at the higher filter frequency, whereas filtering at 500 Hz attenuates this effect. This result suggests a reasonable explanation for the slight correlation found by Labarca et al. (1985), although it does not exclude other possibilities. In any case, it will be interesting to study in more detail the fast flickering process that leads to the high open-channel noise in CLC-0 (Läuger, 1985).

Using the concatameric WT/mutant constructs, we were able to test for the obedience of the microscopic reversibility restricted to transitions of the fast gate. No violation of

microscopic reversibility was detected. How does this relate to earlier data on wild-type CLC-0? Single-channel analysis of the native *Torpedo* Cl^- channel revealed a time asymmetry of gating transitions and thus a violation of microscopic reversibility: after long (slow gate) closures, channels often activate by simultaneous opening of both pores. Long closures are entered frequently from the intermediate conductance level, where only one pore is open (Richard and Miller, 1990). We now can exclude the possibility that any interaction of fast gating transitions between the individual pores is responsible for the violation of microscopic reversibility. As already suggested by Richard and Miller (1990), it is the interaction between fast and slow gating that leads to the violation of detailed balance in CLC-0 single-channel traces.

From the complete independence of the conformational changes that lead to opening and closing of single protopores of the state of the physically attached pore, as suggested by our results, one might speculate that these conformational changes involve only minor movements of the protein structure. Such a small rearrangement might argue against fast gating models in which opening is associated with large changes in the electrostatics seen by ions that are present in the pore (Chen and Miller, 1996). More experiments are needed, however, to clarify the kind of conformational change that is associated with fast gating.

This work was supported by grants from the Deutsche Forschungsgemeinschaft and from the Fonds der Chemischen Industrie.

REFERENCES

Bauer, C. K., K. Steinmeyer, J. R. Schwarz, and T. J. Jentsch. 1991. Completely functional double-barreled chloride channels expressed from a single *Torpedo* cDNA. *Proc. Natl. Acad. Sci. USA.* 88: 11052–11056.

Chen, T.-Y., and C. Miller. 1996. Nonequilibrium gating and voltage dependence of CLC-0 Cl^- channel. *J. Gen. Physiol.* 108:237–250.

Fisher, S. E., G. C. M. Black, S. E. Lloyd, E. Hatchwell, O. Wrong, R. V. Thakker, and I. W. Craig. 1994. Isolation and partial characterization of a chloride channel gene which is expressed in kidney and is a candidate for Dent's disease (an X-linked hereditary nephrolithiasis). *Hum. Mol. Genet.* 3:2053–2059.

George, A. L., Jr., M. A. Crackower, J. A. Abdalla, A. J. Hudson, and G. C. Ebers. 1993. Molecular basis of Thomsen's disease (autosomal dominant myotonia congenita). *Nature Genet.* 3:305–310.

Gründer, S., A. Thiemann, M. Pusch, and T. J. Jentsch. 1992. Regions involved in the opening of CLC-2 chloride channel by voltage and cell volume. *Nature.* 360:759–763.

Hamill, O. P., A. Marty, E. Neher, B. Sakman, and F. J. Sigworth. 1981. Improved patch-clamp techniques for high-resolution current recording from cells and cell-free membrane patches. *Pflügers Arch.* 391:85–100.

Hanke, W., and C. Miller. 1983. Single chloride channels from *Torpedo* electroplax. Activation by protons. *J. Gen. Physiol.* 82:25–42.

Jentsch, T. J. 1996. Chloride channels. A molecular perspective. *Curr. Opin. Neurobiol.* 6:303–310.

Jentsch, T. J., W. Günther, M. Pusch, and B. Schwappach. 1995. Properties of voltage-gated chloride channels of the CLC gene family. *J. Physiol. (Lond.).* 482P:19S–25S.

Jentsch, T. J., K. Steinmeyer, and G. Schwarz. 1990. Primary structure of *Torpedo marmorata* chloride channel isolated by expression cloning in *Xenopus* oocytes. *Nature.* 348:510–514.

Koch, M. C., K. Steinmeyer, C. Lorenz, K. Ricker, F. Wolf, M. Otto, B. Zoll, F. Lehmann-Horn, K.-H. Grzeschik, and T. J. Jentsch. 1992. The skeletal muscle chloride channel in dominant and recessive human myotonia. *Science.* 257:797–800.

Labarca, P., J. A. Rice, D. R. Fredkin, and M. Montal. 1985. Kinetic analysis of channel gating. Application to the cholinergic receptor channel and the chloride channel from *Torpedo californica. Biophys. J.* 47:469–478.

Läuger, P. Structural fluctuations, and current noise of ionic channels. 1985. *Biophys. J.* 48:369–373.

Lloyd, S. E., S. H. S. Pearce, S. E. Fisher, K. Steinmeyer, B. Schwappach, S. J. Scheinmann, B. Harding, A. Bolino, M. Devoto, P. Goodyer, S. P. A. Rigden, O. Wrong, T. J. Jentsch, I. W. Craig, and R. V. Thakker. 1995. Mutations in the chloride channel CLC-5 are associated with X-linked hypercalciuric nephrolithiasis. *Nature.* 379:445–449.

Ludewig, U., T. J. Jentsch, and M. Pusch. 1997. Analysis of a protein region involved in permeation and gating of the voltage-gated *Torpedo* chloride channel CLC-0. *J. Physiol. (Lond.).* 498:691–702.

Ludewig, U., M. Pusch, and T. J. Jentsch. 1996. Two physically distinct pores in the dimeric chloride channel CLC-0. *Nature.* 383:340–343.

Middleton, R. E., D. J. Pheasant, and C. Miller. 1996. Homodimeric architecture of a CLC-type chloride ion channel. *Nature.* 383:337–340.

Miller, C. 1982. Open-state substructure of single chloride channels from *Torpedo* electroplax. *Philos. Trans. R. Soc. Lond. B.* 299:401–411.

Miller, C., and M. M. White. 1984. Dimeric structure of single chloride channels from *Torpedo* electroplax. *Proc. Natl. Acad. Sci. USA.* 81: 2772–2775.

Pusch, M., and T. J. Jentsch. 1994. Molecular physiology of voltage-gated chloride channels. *Physiol. Rev.* 74:813–827.

Pusch, M., U. Ludewig, and T. J. Jentsch. 1997. Temperature dependence of fast and slow gating relaxations of CLC-0 chloride channels. *J. Gen. Physiol.* 109:105–116.

Pusch, M., U. Ludewig, A. Rehfeldt, and T. J. Jentsch. 1995. Gating of the voltage-dependent chloride channel CLC-0 by the permeant anion. *Nature.* 373:527–531.

Richard, E. A., and C. Miller. 1990. Steady-state coupling of ion-channel conformations to a transmembrane ion gradient. *Science.* 247: 1208–1210.

Sigworth, F. J., and S. M. Sine. 1987. Data transformation for improved display and fitting of single channel dwell time histograms. *Biophys. J.* 52:1047–1054.

Staley, K., R. Smith, J. Schaack, C. L. Wilcox, and T. J. Jentsch. 1996. Alteration of $GABA_A$ receptor function following gene transfer of the CLC-2 chloride channel. *Neuron.* 17:543–551.

Steinmeyer, K., R. Klocke, C. Ortland, M. Gronemeier, H. Jokusch, S. Gründer, and T. J. Jentsch. 1991a. Inactivation of muscle chloride channel by transposon insertion in myotonic mice. *Nature.* 354: 304–308.

Steinmeyer, K., C. Lorenz, M. Pusch, M. C. Koch, and T. J. Jentsch. 1994. Multimeric structure of CLC-1 chloride channels as revealed by mutations in dominant myotonia congenita (Thomsen). *EMBO J.* 13: 737–743.

Steinmeyer, K., C. Ortland, and T. J. Jentsch. 1991b. Primary structure and functional expression of a developmentally regulated skeletal muscle chloride channel. *Nature.* 354:301–304.

Steinmeyer, K., B. Schwappach, M. Bens, A. Vandewalle, and T. J. Jentsch. 1995. Cloning and functional expression of rat CLC-5, a chloride channel related to kidney disease. *J. Biol. Chem.* 270:31172–31177.